Microsyst Technol (2020) 26:3063–3068
DOI 10.1007/s00542-017-3622-3

TECHNICAL PAPER

Highly sensitive refractive index sensor based on degeneracy in specialty optical fibers: a new approach

Arpan Roy[1] · Abhijit Biswas[1] · R. K. Varshney[2] · Somnath Ghosh[3]

Received: 2 August 2017 / Accepted: 3 November 2017 / Published online: 9 November 2017
© Springer-Verlag GmbH Germany, part of Springer Nature 2017

Abstract We study the phenomenon of deliberate intermodal interactions in a specially designed index guided Microstructured Optical Fiber (MOF) by exploiting multipole expansion method (White et al. 2002). The MOF is designed in such a way that the first layer of holes is judiciously filled with a material having refractive index slightly greater than the background material or core and remaining holes are filled with air. Accordingly, we find an interesting phenomenon of mode crossing between the fundamental mode and a targeted defect mode while tuning the wavelength. Exploring this transition wavelength of the mode crossing, we propose a design of a fiber optic sensor for refractive index measurement (Silva et al. 2014) with enhanced sensitivity.

1 Introduction

The discovery of photonic crystal fiber or microstructured optical fiber (Russell et al. 1996) opens up tremendous opportunity for the researchers to overcome many constraints of conventional optical fibers, owing to their unique properties such as endlessly single mode operation with large core area (Birks et al. 1997; Knight et al. 1998), low bend-loss sensitivity (Wheeler et al. 2014), polarization maintaining capabilities (Kaczmarek 2014), and many more. The MOF consists of a periodic arrangement of air holes with triangular or hexagonal symmetry running along their entire length, together with a missing air hole or a low refractive index material at the center acting as the core. Due to the special geometry of MOFs, they host a range of unique capabilities which would be exploited especially for enhanced sensing applications such as refractive index sensor, pressure sensor, high-temperature sensor, etc. Lately, refractive index sensors based on MOFs have been explored widely in the field of chemical and biological detection industry; for example, fuel quality measurement (Osorio et al. 2013), measurement of salinity of water (Pereira et al. 2004; Adhikari et al. 2015), etc. Moreover, this technology has also been effectively applied in detection of drugs/DNA interaction, and cell growth (Zibaii et al. 2010a, b). Many of these MOF based sensors rely on photonic bandgap (PBG) properties or generic resonant coupling phenomena in dual core MOF where the concept of dual core was achieved by selectively filling the cladding air holes (Darran et al. 2009; Luan et al. 2016; Town et al. 2010).

In 2004, Kim et al. through their numerical investigations established that presence of a thin silica ring surrounding the air core of a photonic bandgap fiber introduces surface modes (Kim et al. 2004), unlike in a conventional optical fiber counterpart. In this context, M. J. F. Digonnet verified the existence of surface modes in a circular air-core photonic bandgap fiber with triangular symmetry in the surrounding cladding (Digonnet et al. 2004). These surface modes or defect modes are present at the boundary between the core and the holey cladding. Judicious choice of structural parameters creates a condition where the effective index difference between the supported fundamental mode and deliberate defect mode

✉ Somnath Ghosh
somiit@rediffmail.com

[1] Institute of Radio Physics and Electronics, University of Calcutta, Kolkata 700009, India

[2] Department of Physics, Indian Institute of Technology Delhi, New Delhi 110016, India

[3] Department of Physics, Indian Institute of Technology Jodhpur, Rajasthan 342011, India

would be negligibly small, which essentially leads to an interaction among the chosen modes. The wavelength dependence of this modal interaction dynamics and parametric dependence of this feature would be promising in device level applications, particularly for label-free sensing based on frequency splitting.

In this paper, we design a specialty MOF with customized index profile by suitably tailoring the index value of the first cladding ring, unlike the background system. The proposed advanced cladding layer consists of a material having slightly higher refractive index than the core index in the first layer of holes, thereby breaking the radial symmetry of the over-all cladding. Previously, this W-type index profile was used in some interesting applications including dispersion compensation both in conventional fibers and MOF's (Thyagarajan et al. 1996; Varshney et al. 2005). In this work, we have done the modal analysis and investigated their interactions in the proposed MOF. The optimized MOF geometry supports the defect mode with a slightly higher effective index than the fundamental mode; hence they interact with each other as the operating condition is tuned. Judicious tailoring and control of the modal interaction lead to significant power switching between the modes and hence in the output. Detecting the sensitivity of this power splitting at the output and investigating its parametric control, we propose a new MOF based refractive index sensor (Efendioglu 2017).

2 Theory and proposed scheme

In the MOF, the light wave is guided through manipulation of the waveguide geometry rather than the index of refraction itself. Depending on the index of the core material, the MOF can be classified into two categories either as photonic bandgap fiber, or index guided fiber. In the photonic bandgap fiber, the core region consists of air or of a material having a refractive index lower than the effective refractive index of the cladding region and in general the diameter of the core is greater than that of the cladding air holes. An index guided MOF accommodates a missing air hole at the center acting as the core of the MOF that is surrounded by a silica matrix with hexagonal/circular periodic array of air-hole inclusions forming the effective cladding layer. The effective index of the cladding is given by β_{FSM}/k, where β_{FSM} is the propagation constant of the fundamental space filling mode (FSM) and k $(= 2\pi/\lambda)$ is the free space propagation constant with λ being the wavelength. Here FSM is the fundamental space filling mode of the infinite photonic crystal cladding. As the cladding layers consist of both air and silica material, therefore the average index of the cladding becomes lower than the core, which is entirely silica based. This condition satisfies the working principle for the conventional optical fibers. Here light is guided through modified total internal reflection *akin* total internal reflection in conventional step index fiber. It is well understood that in a conventional optical fiber if the core index (n_1) is very close to cladding index (n_2) then weakly guiding approximation or scalar wave approximation can be implemented. In this approximation, the propagation constant of transverse electric (*TE*) and transverse magnetic (*TM*) modes are nearly equal and thus they are usually referred to as linearly polarized or *LP* modes. Under weakly guiding approximation, the transverse component of electric field satisfies the scalar wave equation, and from the solution to this equation it is found that for a mode having effective index in between the indices of the core and cladding will remain oscillatory or sustain in the core region known as the guided mode; and those modes having effective index lower than the cladding index will remain oscillatory in the cladding region. Introducing a deliberate defect may excite a defect mode in an otherwise periodic cladding.

In the present work, we specially design a MOF to achieve the condition of weakly guiding approximation by introducing a material with a slightly higher refractive index than silica in the first layer of air holes in the cladding of the MOF. The effective refractive index profile of the index-guided MOF is obtained by using effective index method, which is essentially the average value of refractive index of the background material and the material of the hole taking into account their respective area. Under this condition, since the refractive index difference between the core and cladding is very small, the effective indices of the core and cladding guided modes come close to each other and any further interaction leads to mode Variation of real part ofcrossing in the dual mode structure. This phenomenon of mode crossing is exploited to design a refractive index sensor. Using our design scheme and proposed fiber, we plan to feed the output of an optical source over a wide range of operational wavelengths to the designed MOF and the output is to be detected by an optical detector. Then tuning the wavelength of a source continuously, a condition can be achieved where the output beam power will be changed drastically manifesting the onset of mode crossing. Then by detecting this power transition wavelength, the refractive index of the hole filling material (here high concentration of sugar solution, benzene, toluene, styrene) can be determined.

3 Fiber design and performance evaluation

In our proposed fiber design, we have optimized a set of fiber parameters and also introduced a material in the first layer of the cladding holes in silica matrix to achieve mode crossing

between the fundamental mode and the defect mode. We optimize three layers of holes, each with equal radius surrounding the core with hexagonal symmetry, which are embedded in the silica matrix. To reduce the index contrast between the core and cladding, a material with refractive index of 1.46 is incorporated in the first layer of the cladding holes. The refractive index profile of the designed MOF structure is shown in Fig. 1. The wavelength dependence of refractive index for silica is obtained by using the *Sellmeier* relationship, however for the proposed range of wavelength; we have ignored the wavelength dependency of refractive index for the first layer of holes. Modal analysis and related numerical calculations are carried out using the *CUDOS*®, which is based on multipole expansion method, and post-processed in *MATLAB*®. During optimization of the MOF structure, it was noticed that the difference between effective indices of guided mode and defect mode decreases with the reduction of pitch (Λ, center-to-center air hole separation). To reduce the material index contrast between the core and cladding, we increase the radius of the filled holes. However, with this particular modification, material-filled holes with a larger radius itself support the local guided mode. Accordingly, we optimize the hole-radius such that it does not guide any isolated mode. Having carried out rigorous optimization, a highly sensitive mode crossing is achieved numerically for the structure having the pitch (Λ) of 1.9 μm, air hole radius of 0.15 μm and hole-diameter to pitch ratio (d/Λ) of 0.158 at 590.9 nm. It is observed that it supports two modes; one is core-guided mode and the other is defect mode in the cladding. Their field profiles at a wavelength of 592 nm are shown in Fig. 2. From this figure, it is evident that the core mode has maximum field intensity at the center while the defect mode has field intensity in the form of a circular ring around the core having no power confined in the core. Propagation constants of these modes are complex. Variation of real parts of the effective index (n_{eff}) of these modes with wavelength is shown in Fig. 3, where red curve marks core mode and blue for defect mode. It is evident from the curve that the real part of n_{eff} for the core mode decreases rapidly with decrease in wavelength, whereas the real part of n_{eff} for defect mode increases negligibly. At wavelength of 590.9 nm the modes cross each other. Hence, for wavelengths below 590.9 nm, the defect mode acts as the fundamental mode in our structure. The variation of imaginary part of n_{eff} with wavelength for both core-guided mode and defect mode is displayed in Fig. 4. For this case also we identify the phenomenon of mode crossing when the modes exchange their lifetime around the degeneracy point. From waveguide theory, it is well understood that the waveguide loss is directly proportional to the imaginary part of n_{eff}. Hence, for the optimized fiber geometry with the chosen parameters, the real and imaginary parts of effective index variation show crossing behavior resulting in an over-all mode crossing behavior. Figure 5 shows the variation of fractional power distribution between the interacting core and defect modes with wavelength for the designed fiber discussed above. In the longer range of operating wavelengths relative to the mode crossing, most of the power confined in the core mode while at wavelengths below the mode crossing wavelength power mainly remains in the cladding. From the application point of view, this mode-crossing wavelength can be detected by simply placing an optical detector at the core region (near field) rather than an optical spectrum analyzer which will reduce the cost of detection.

Accordingly, we fill the first layer of holes with different refractive indices and calculate the mode crossing wavelength. The variation in mode crossing wavelength with

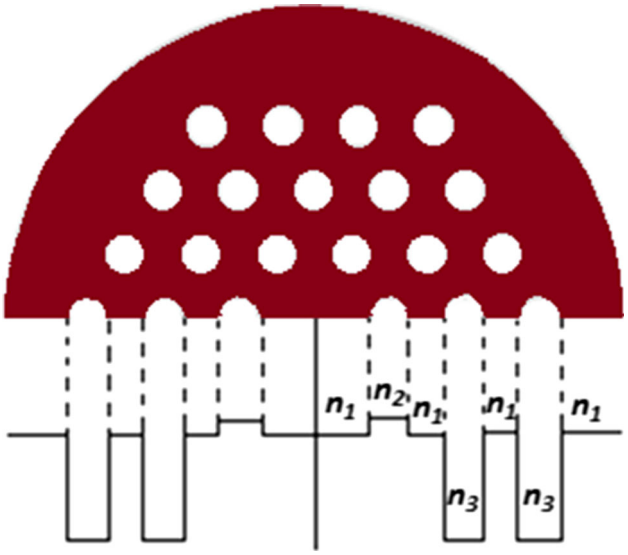

Fig. 1 Schematic refractive index profile of the proposed MOF. Cladding consists of three rings of holes (white circles) with triangular/hexagonal symmetry embedded in silica matrix (brown background).The first layer is filled with a material having refractive index 1.46

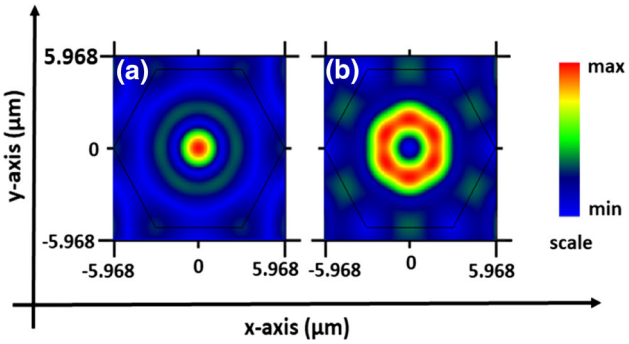

Fig. 2 Field profiles of (**a**) core-guided mode and (**b**) defect guided mode

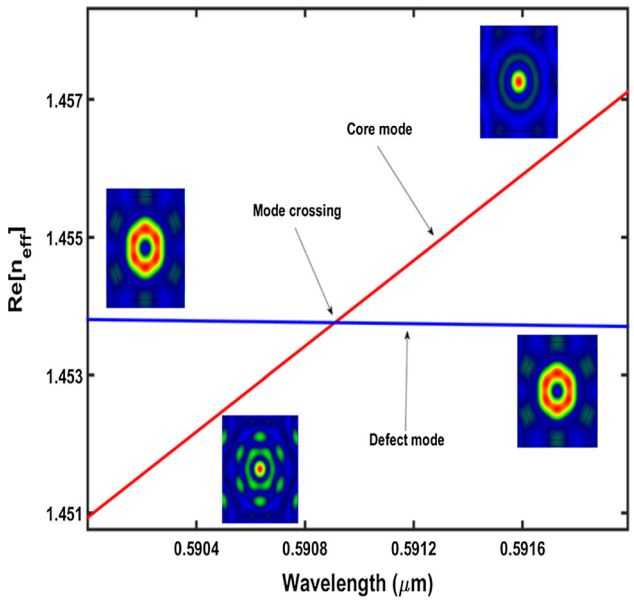

Fig. 3 Variation of real part of n_{eff} with operating wavelength for both core-guided mode and defect mode. The MOF structure features pitch $(\Lambda) = 1.9$ μm, $d/\Lambda = 0.158$ and the first layer of holes is filled with a material having index of 1.46

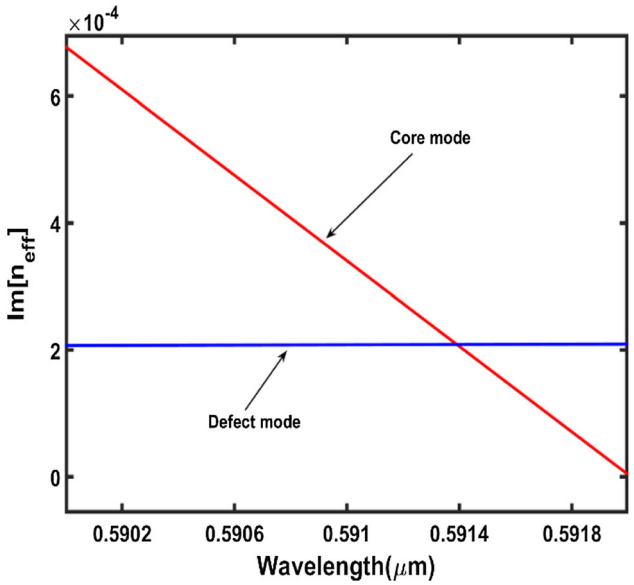

Fig. 4 Variation of imaginary part of n_{eff} with operating wavelength for both core-guided mode and defect mode. The MOF structure features pitch $(\Lambda) = 1.9$ μm, $d/\Lambda = 0.158$ and the first layer of holes is filled with a material having index of 1.46

various hole filling material indices is shown in Fig. 6. Hence we intend to vThe MOF structure features

ary hole filling material index from 1.46 to 1.50 with an index step of 0.005. This clearly indicates that at the smaller value of the refractive index (n_f) of hole filling material, the crossing wavelength increases slowly with n_f, however, this change is relatively larger at a higher value

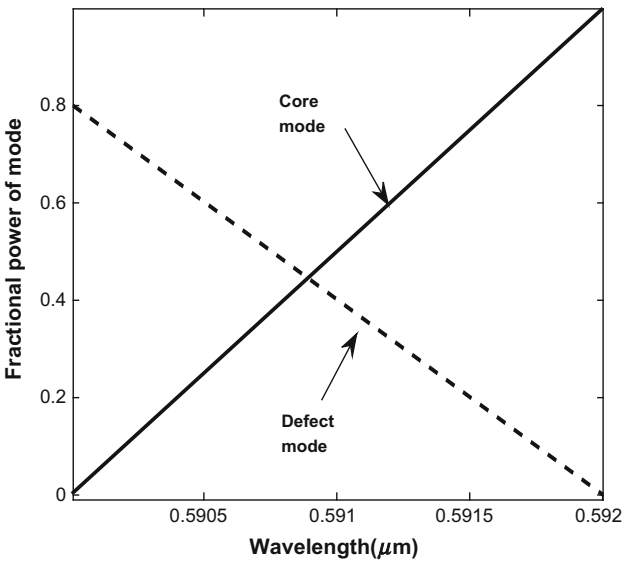

Fig. 5 Tunability of fractional power distribution with operating wavelength

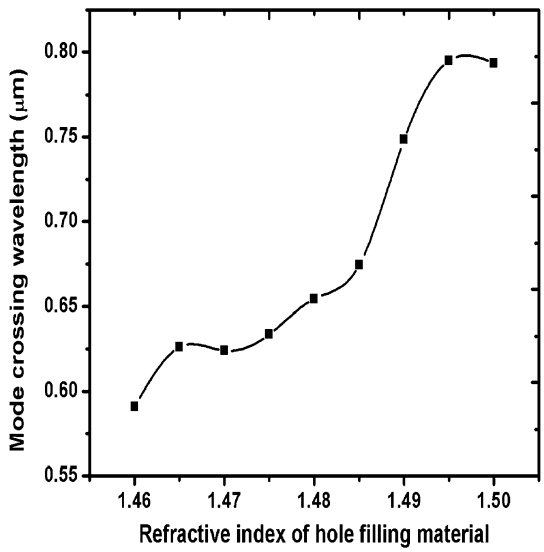

Fig. 6 Dependence of mode-crossing wavelength with index of hole filling material

of n_f. Thus such a shift in crossing wavelength with index change could be exploited in sensing applications. The sensitivity (S_λ) of a refractive index sensor can be obtain by using the following relation.

$$S_\lambda = \partial\lambda(n)/\partial n \tag{1}$$

where $\partial\lambda(n_f)$ is the change in mode-crossing wavelength. In Fig. 7 we demonstrate the variation in sensitivity with the hole filling material refractive indices. From our analysis, it is observed that the sensitivity attains its maximum value of 12,000 nm/RIU when a hole filling material refractive index is 1.49. The MOF based RI sensor can

broadly be classified in two categories as the interferometric and resonance-based MOF configurations. In Park et al. (2010) realized a PCF-based reflection type refractometer for RI measurement with sensitivity 850 nm/RIU. Moreover, Silva et al. 2011 developed a refractometer based on multimodal interference with sensitivity 800 nm/RIU. Sun et al. 2011 proposed a new concept of dual-core PCF sensor based on a conventional solid core as well as a microstructured core with a sensitivity of 8500 nm/RIU. A detail development history of optical fibre based RI sensor can be obtained from (Silva et al. 2014). From our analysis, it is observed that the sensitivity attains its maximum value of 12,000 nm/RIU.

To address the fabrication feasibility of our optimized fiber geometry, the tolerance is tested by estimating the sensitivity for the structures having larger and smaller radii of the first layer of holes and the relevant results are shown in Fig. 8. Our findings reveal that the maximum sensitivity remains almost constant with the reduction of holes radius about 5% whereas the sensitivity decreases drastically with the increment of hole radius. Moreover, the increment of holes radius by 2% decreases the maximum sensitivity by 17%. To summarize, the point of maximum sensitivity is affected by a small value due to the change of hole radii of the first layer.

For device level implementation of this proposed sensing scheme, we study the effect of deliberate scaling of the MOF cross-section by varying all its parameters like pitch, hole diameters in a fixed proportion. Hence we consider up and down scaling in the MOF cross section by multiplying its cross section parameters by factors 1.05 and 0.95, respectively (Russell et al. 2006).

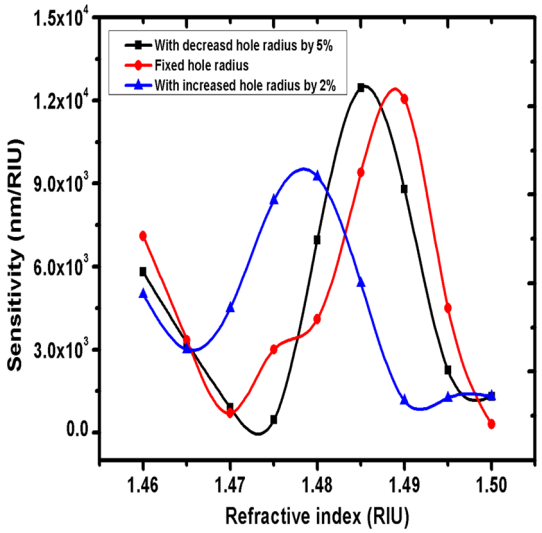

Fig. 8 Variation of sensitivity with hole filling material index for different hole radii

The sensitivity behavior of the newly formed structures is displayed in Fig. 9. There is a shifting if the maximum sensitivity peaks with up and down tapered structures with respect to normal structure as well as there is a change in maximum sensitivity. For up scaled cross-section, the sensitivity is enhanced whereas down scaled structure exhibits the contrary. This result could be useful to choose the high sensitivity region of a refractive index sensor, while a longitudinally tapered fiber optic head is optimized. Moreover, the sensitivity remains almost unchanged when dispersive nature of refractive indices is considered.

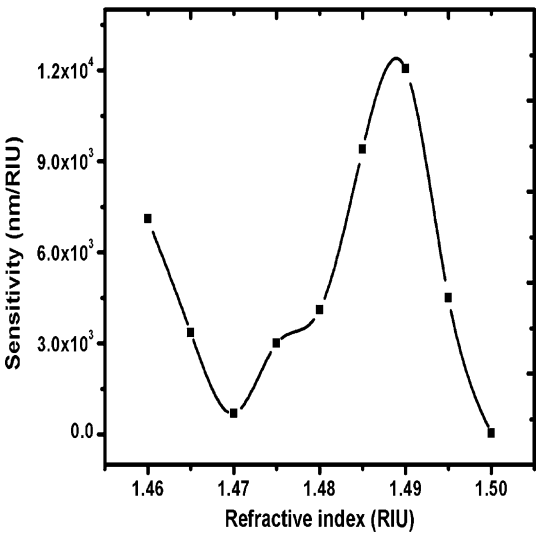

Fig. 7 Dependence of sensitivity with hole filling material index

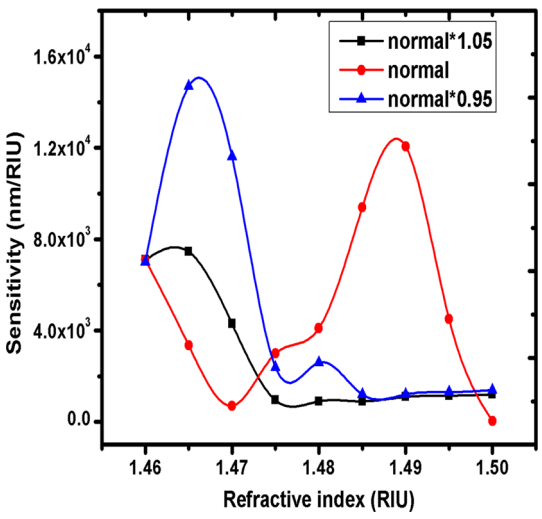

Fig. 9 Sensitivity after up and down tapered cross-section of the MOF structure by a factor 1.05 and 0.95, respectively

4 Conclusion

In conclusion, we have proposed a new scheme for enhanced refractive index sensing. The proposal has been implemented to optimize a specialty index guided microstructured optical fiber with enhanced sensitivity to index variation in the air holes of the cladding. Our detailed numerical study exhibited the phenomenon of mode crossing between the core-guided mode and deliberate defect mode. The variation of mode crossing wavelength with hole-filling material index is demonstrated. The proposed MOF geometry with its highly sensitive mode switching behavior could be utilized for fiber optic frequency splitting based label free detectors and devices.

Acknowledgements SG acknowledges the financial support from the Department of Science and Technology, India, IFA-12, PH-23.

References

Adhikari BR, Govindhan M, Chen A (2015) Carbon nanomaterials based electrochemical sensors/biosensors for the sensitive detection of pharmaceutical and biological compounds. Sensors 15:22490–22508

Birks TA, Knight JC, Russell PSJ (1997) Endlessly single-mode photonic crystal fiber. Opt Lett 22:961

Digonnet MJF, Kim HK, Shin J, Fan S, Kino GS (2004) Simple geometric criterion to predict the existence of surface modes in air-core photonic-bandgap fibers. Opt Exp 12:1864–1872

Efendioglu HS (2017) A review of fiber-optic modal modulated sensors: specklegram and modal power distribution sensing. IEEE Sens J 17(7):2055–2064

Kaczmarek C (2014) Polarization-maintaining photonic crystal fiber modal interferometer. In: Proc. SPIE 9291, 13th International scientific conference on optical sensors and electronic sensors, 92910G, August 19

Kim HK, Shin J, Fan S, Digonnet MJF, Kino GS (2004) Designing air-core photonic-bandgap fibers free of surface modes. IEEE J Quantum Electron 40:551–556

Knight JC, Birks TA, Cregan RF, Russell PSJ, Sandro JPD (1998) Large mode area photonic crystal fibre. Electron Lett 34(13):1347–1348

Luan N, Ding C, Yao J (2016) A refractive index and temperature sensor based on surface plasmon resonance in an exposed-core microstructured optical fiber. IEEE Photonics J 8(2):1–8

Osorio JH, Mosquera L, Gouveia CJ, Biazoli CR, Hayashi JG, Jorge PAS, Cordeiro CMB (2013) High sensitivity LPG Mach-Zehnder sensor for real-time fuel conformity analysis. Meas Sci Technol 24:015102

Park KS, Choi HY, Park SJ, Paek UC, Lee BH (2010) Temperature robust refractive index sensor based on a photonic crystal fiber interferometer. IEEE Sens J 10:1147–1148

Pereira DA, Frazão O, Santos JL (2004) Fibre Bragg grating sensing system for simultaneous measurement of salinity and temperature. Opt Eng 43:299–304

Russell PS (2006) Photonic-crystal fibers. J Light Technol 24(12):4729–4749

Russell PStJ, Atkin DM, Birks TA, Roberts PJ (1996) Bound modes of two-dimensional photonic crystal waveguides. In: Rarity JG, Weisbuch C (eds) Quantum optics in wavelength scale structures. Kluwer Academic Press, pp 203–219

Silva S, Santos JL, Malcata FX, Kobelke J, Schuster K, Frazão O (2011) Optical refractometer based on large-core air-clad photonic crystal fibers. Opt Lett 36:852–885

Silva S, Roriz P, Frazão O (2014) Refractive index measurement of liquids based on microstructured optical fibers. Photonics 1:516–529

Sun B, Chen MY, Zhang YK, Yang JC, Yao JQ, Cui HX (2011) Microstructured-core photonic-crystal fiber for ultra-sensitive refractive index sensing. Opt Exp 19:4091–4100

Thyagarajan K, Varshney RK, Palai P, Ghatak AK, Goyal IC (1996) A novel design of a dispersion compensating fiber. IEEE Photonics Tech Lett 8:1510–1512

Town GE, Yuan W, McCosker R, Bang O (2010) Microstructured optical fiber refractive index sensor. Opt Lett 35:856–858

Varshney SK, Saitoh K, Koshiba M (2005) A novel design for dispersion compensating photonic crystal fiber Raman amplifier. IEEE Photonics Technol Lett 17(10):2062–2064

Wheeler NV, Heidt AM, Baddela NK, Fokoua EN, Hayes JR, Sandoghchi SR, Poletti F, Petrovich MN, Richardson DJ (2014) Low-loss and low-bend-sensitivity mid-infrared guidance in a hollow-core–photonic-bandgap fiber. Opt Lett 39:295–298

White TP, Kuhlmey BT, McPhedran RC, Maystre D, Renversez G, Sterke CM, Botten LC (2002) Multipole method for microstructured optical fibers. I. Formulation. J Opt Soc Am B 19:2322–2330

Wu DKC, Boris TK, Benjamin JE (2009) Ultrasensitive photonic crystal fiber refractive index sensor. Opt Lett 34:322–324

Zibaii MI, Kazemi A, Latifi H, Azar MK, Hosseini SM, Ghezelaiagh MH (2010a) Measuring bacterial growth by refractive index tapered fiber optic biosensor. J Photochem Photobiol B 3:313–320

Zibaii MI, Latifi H, Karami M, Gholami M, Hosseini SM, Ghezelayagh MH (2010b) Non-adiabatic tapered optical fiber sensor for measuring the interaction between alpha-amino acids in aqueous carbohydrate solution. Meas Sci Technol 21:10580